
MOLECULAR SPECTROSCOPY

Particular Features of the $\nu(\text{OH})$ Absorption Band of Strongly Hydrogen-Bonded Complexes in the Gas Phase, Low-Temperature Matrices, and Crystalline Films at 12–600 K

R. E. Asfin*, G. S. Denisov*, Z. Mielke**, and K. G. Tokhadze*

* *Institute of Physics, St. Petersburg State University, Peterhof, St. Petersburg, 198504 Russia*

** *Faculty of Chemistry, University of Wrocław, 50-383 Wrocław, Poland*

Received September 6, 2004

Abstract—The particular features of the $\nu(\text{OH})$ absorption band of dimers with a strong hydrogen bond ($\Delta H = 24\text{--}50\text{ kcal/mol} = 8000\text{--}17000\text{ cm}^{-1}/\text{molecule}$) formed by molecules of phosphinic acids R_2POOH N_2 are studied in the gas phase, low-temperature argon and nitrogen matrices, and crystalline films. It is found that, irrespective of the type of the acid, the $\nu(\text{OH})$ IR absorption bands of dimers are broad ($\Delta\nu_{1/2} \sim 1000\text{ cm}^{-1}$) and similar in shape, exhibiting a characteristic ABC structure. The formation of these anomalously broad absorption bands is shown to be primarily associated with vibrations of the $-\text{POOH}$ fragments, participating in the hydrogen bonding. A change in the temperature in the range 12–600 K and the passage from cyclic dimers in the gas phase to helical chains with hydrogen bonds in the crystalline state cause no significant changes in the shape, width, or structure of the dimer band. The contribution to the formation of the broad absorption band of the $(\text{R}_2\text{POOH})_2$ dimers made by anharmonic interactions between the high-frequency $\nu(\text{OH})$ vibration and the low-frequency intermolecular vibrations is estimated. The absorption spectra of weak complexes $\text{R}_2\text{POOH}\dots\text{N}_2$ in matrices at 12 K are discussed. © 2005 Pleiades Publishing, Inc.

INTRODUCTION

A large width and a peculiar structure of the absorption band of the $\nu(\text{AH})$ stretching vibration of a hydrogen-bonded complex $\text{AH}\dots\text{B}$ is one of the most complex phenomena in spectroscopy of intermolecular interactions, an exhaustive account of which has yet to be offered. Certain progress has been made in recent years only in the description of the shape and structure of the bands of not-too-strong complexes $\text{B}\dots\text{HHal}$ in the gas phase [1–4], in which anharmonic interactions between the high-frequency $\nu(\text{HH})\text{al}$ vibration and the low-frequency intermolecular vibrations play a dominant role, leading to the appearance of hot and combination transitions and to strong vibrational–rotational interactions. For these systems, a satisfactory agreement between the theory and experiment was obtained in terms of both semiempirical [5] and nonempirical [6] models.

The analysis of the band shape of complexes whose formation involves the participation of polyatomic proton donors $-\text{OH}$ and $-\text{NH}$ is much more complex. The most general factor determining, in one way or another, the formation of the absorption band shapes of these complexes is the resonance interaction between the $\nu(\text{AH})$ stretching vibration of a hydrogen bond and the vibrational modes of a proton donor. Models proposed by different authors deal with particular systems and,

therefore, have a limited range of applicability [7–11]. The majority of these studies are devoted to the analysis of the $\nu(\text{OH})$ band in complexes with the $\text{OH}\dots\text{O}$ bond; however, they do not have a universal character since, even phenomenologically, the spectral properties of hydrogen bridges of this type differ markedly from the properties of other systems. In particular, it seems that special attention is necessary in describing the $\nu(\text{NH})$ band contour in molecular and ionic complexes with the $\text{NH}\dots\text{B}$ bond, whose structure is frequently especially complex and branched [12–15].

Systematization of the results of measurements of the vibrational spectra, structure, and thermodynamic parameters of hydrogen-bonded systems made it possible to formulate empirical correlation relations between their spectral, geometrical, and energetic characteristics [16–19]. It was found that, with increasing hydrogen bond energy ΔH , the low-frequency shift of the $\nu(\text{AH})$ band, as well as the integrated intensity and the width (the second spectral moment) of this band, increases. These relations were obtained on the basis of data about weak and moderate hydrogen bonds, and they, of course, play an important role in testing theoretical models. However, not all of these models were obtained under conditions of minimal interactions with the medium, i.e., in the gas phase, molecular beams, or inert low-temperature matrices. At the same time, it is

such experiments that are especially important in developing theoretical models. Furthermore, there are some grounds to believe that, in the case of stronger hydrogen bonds with a greater covalent contribution, these correlation relations will be violated. In particular, a difficult problem is the analysis of the nature of the $\nu(\text{AH})$ band contour in complexes with a strong hydrogen bond whose energy approaches the energy of valence bonds and that is classified as a three-center four-electron bond. In such systems, the potential of the longitudinal motion of a proton has two minima of similar depth, with the height of the barrier between them being comparable to the energy of the zeroth vibrational level. Apart from the considerable anharmonicity, the spectral parameters of the $\nu(\text{AH})$ band are affected in this case by the delocalization of a proton migrating between two, generally nonequivalent, positions in the hydrogen bridge. Experiment shows that the structure of such a complex is very sensitive to external actions; for example, both the vibrational spectrum of the $\text{HalH}\dots\text{NH}_3$ complex in a low-temperature matrix and the position of a proton in the complex change qualitatively in the series of matrix gases from neon to xenon [20–23]. This means that, in constructing models, experimental data obtained for one and the same system in different conditions (from the gas phase to the crystalline state) are of vital importance.

The strongest hydrogen bonds are observed in ion-molecular complexes of the $(\text{AHA})^-$ and $(\text{BHB})^+$ types [24–26]; however, it is especially difficult to study the spectral properties of charged complexes under conditions of weak interactions with the medium, and, for the time being, such studies are few. In neutral systems, the strongest hydrogen bonds of the $\text{OH}\dots\text{O}$ type are formed in self-associates of phosphinic and, seemingly, arsonic acids [27–29], and it is only due to the high thermal stability of these associates that one is able to observe their IR spectra in the gas phase at temperatures within 400–600 K, at which cyclic dimers are in equilibrium with monomeric molecules [30–33]. This made it possible to perform direct measurements of the energy of the hydrogen bond ($\Delta H = 12\text{--}25$ kcal/mol per bond) and to analyze the temperature dependence of the contour of the $\nu(\text{OH})$ band, which serves as an important criterion in the choice of theoretical models. The parameters of this broad band and its shape turned out to be almost independent of the bonding energy and temperature. It can be noted that, even in the case of carboxylic acids ($\Delta H = 6\text{--}8$ kcal/mol per bond), upon passage from the spectra in the gas phase at $T \sim 300$ K to the spectra measured in molecular beams [34, 35] and low-temperature matrices [36] at $T \sim 10\text{--}12$ K, no significant narrowing of the dimer absorption band is observed, although the structure of this band noticeably sharpens.

In this study, the IR spectra of three phosphinic acids with different dimerization energies are measured in the gas phase, crystalline films, and low-temperature

matrices. The contours of the $\nu(\text{OH})$ band of dimers are compared and analyzed in relation to the phase state and temperature variation in the range 12–600 K.

EXPERIMENTAL

The absorption spectra of the phosphinic acids in the gas phase were obtained using special gas cells adapted for performing measurements in the temperature range 300–750 K. The acid concentration was equal to $(0.6\text{--}3) \times 10^{-3}$ M. In all the experiments, a sample of the substance under study was placed in a cell and then the cell was evacuated to a pressure of $\sim 10^{-2}$ Torr, which was determined by the vapor pressure above the solid substance, and sealed. The cell was placed into a copper heater equipped with KBr windows. The design of the system ensured temperature stability over time and volume within 1–2 K. Cells of two types were used: (i) glass cells with welded sapphire windows 1.6 cm in diameter; the low-frequency transmission limit of these cells was equal to $\nu_M = 1550$ cm^{-1} ; (ii) glass cells with MgF_2 windows 1.3 cm in diameter, which were attached to the cells by means of ceramics. The low-frequency transmission limit of these cells was $\nu_M = 1050$ cm^{-1} . The path length of the cells was in the range from 5 to 8 cm. At high temperatures, the loss of substance in the cells of the second type was somewhat greater; at the same time, with these cells, it was possible to conduct experiments at temperatures as high as 600 K. Most measurements were performed using the cells with sapphire windows, with which we were able to record the $\nu(\text{OH})$ absorption band of monomers and the greater part of the absorption band in the range of the $\nu(\text{OH})$ vibrations of dimers of the acids under study.

The spectra of the phosphinic acids $(\text{CH}_3)_2\text{POOH}$, $(\text{C}_6\text{H}_5)_2\text{POOH}$, and $(\text{CH}_2\text{Cl})_2\text{POOH}$ were obtained in the temperature ranges 370–650, 450–700, and 400–530 K, respectively. For each acid, the lowest temperature of the measurement range is determined by the vapor pressure of this acid at which its absorption spectrum can be reliably measured and the highest temperature depends on the thermal stability of the acid. The gas-phase experiments were described in detail in [30, 32].

The spectra of polycrystalline films of the acids were measured in the temperature range from 80 to 300 K using a standard cryostat with KBr windows. The vapor of the substance under study heated to ~ 400 K was condensed onto a CsI window cooled to 80 K. To remove inhomogeneous broadening from the spectra, the crystalline films were annealed by heating to 250–300 K. After annealing, only reversible temperature changes were observed in the spectra in the range 80–300 K. The spectra of the gas and crystalline phases were measured on a Bruker IFS 28 Fourier spectrometer with a resolution of 1–2 cm^{-1} .

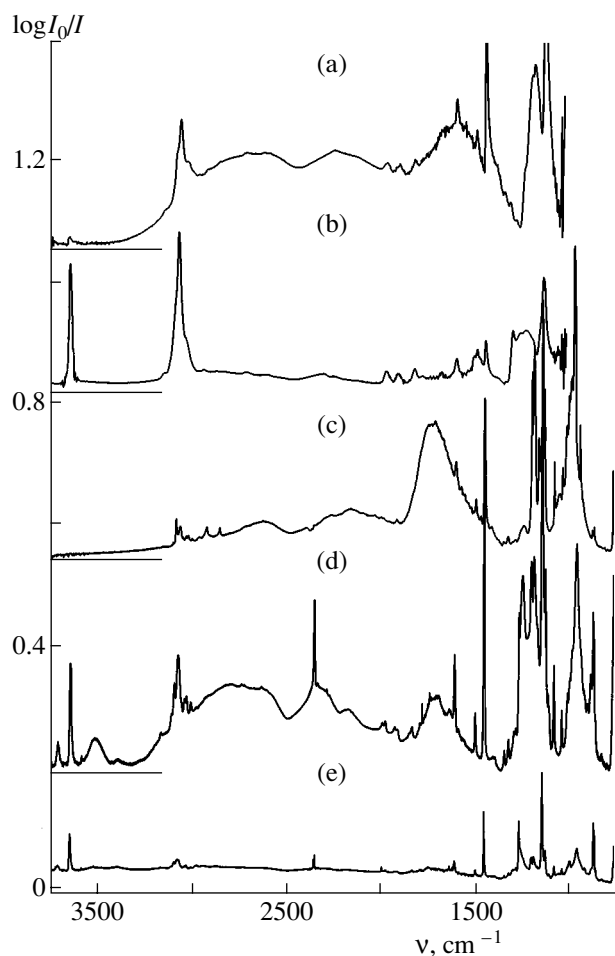


Fig. 1. Absorption spectrum of $(\text{C}_6\text{H}_5)_2\text{POOH}$ in (a, b) the gas phase at $T =$ (a) 490 and (b) 560 K, (c) the solid phase at $T = 100$ K, and (d, e) an argon matrix at $T = 12$ K. See explanations in the text.

The IR spectra of the phosphinic acids in low-temperature (argon or nitrogen) matrices were measured using an Air Products Displex 202A helium cryostat; the experimental procedure was previously described in [37]. Solid samples were placed into stainless steel ampoules, which were evacuated and cooled to ~ 260 K. In the course of the experiments, the vapor of the acid under study and the matrix gas ($M = \text{Ar}, \text{N}_2$), which was supplied via a separate line, were simultaneously deposited onto a gold-plated copper mirror at a temperature within 12–15 K. The acids were evaporated from the ampoules at temperatures within 295–300 $(\text{CH}_3)_2\text{POOH}$, 320–360 $(\text{C}_6\text{H}_5)_2\text{POOH}$, and 315–335 K $(\text{CH}_2\text{Cl})_2\text{POOH}$. Estimations show that, at these temperatures, the relative concentration $R_2\text{POOH}/M$ of the condensed mixtures varies in the range 1/1000–1/200. The spectra were recorded at $T = 12$ K on a Bruker IFS 113v Fourier spectrometer with a resolution of 0.5 cm^{-1} .

RESULTS

The Shape of the $\nu(\text{OH})$ Band of the $(\text{R}_2\text{POOH})_2$ Dimers in the Gas Phase

On an increase in the temperature of the gas cell to 400–450 K, the vapor pressure above the solid sample increases and one can observe the broad $\nu(\text{OH})$ absorption band of dimers of phosphinic acids in the gas phase. As an example, Fig. 1a presents the band of dimers of $(\text{C}_6\text{H}_5)_2\text{POOH}$ recorded using the cell with sapphire windows. Against the background of the broad $\nu(\text{OH})$ band of dimers, located in the range 3500–1100 cm^{-1} , relatively narrow bands associated with fundamental and overtone transitions in the range of framework vibrations of phosphinic acids are observed. In the gas phase, the structure of the band of dimers is characteristic of the band structure of strongly hydrogen-bonded dimers, which consists of the so-called A, B, and C components (bands) [26, 28, 38–40]. At a temperature within the range 470–490 K, the $\nu(\text{OH})$ band of free molecules appears in the spectrum near 3645 cm^{-1} ; the intensity of this band attains a maximum at a temperature of about 540–550 K, at which the broad band of dimers virtually vanishes (Fig. 1b). In the temperature range 300–550 K, the changes in the spectrum are reversible; at $T \approx 600$ K, the acid begins to pyrolyze. The high-temperature absorption spectra of free molecules were used for separating the $\nu(\text{OH})$ absorption band of dimers from the spectrum (Fig. 2). The energies of dimers ΔH of all the acids studied in the gas phase (which, on the whole, exhibit similar temperature dependences of their absorption spectra) were determined previously in [30, 32, 33] from the equilibrium constants of the dimerization reactions $R_2\text{POOH} + R_2\text{POOH} \rightleftharpoons (\text{R}_2\text{POOH})_2$ (Table 1).

In the series of acids under study, the spectral characteristics of the $\nu(\text{OH})$ bands of the monomers are similar to each other. For $(\text{CH}_2\text{Cl})_2\text{POOH}$, $(\text{C}_6\text{H}_5)_2\text{POOH}$, and $(\text{CH}_3)_2\text{POOH}$, the maximum of this band is located at 3640, 3645, and 3650 cm^{-1} , respectively. In the case of the latter acid, this band consists of three strongly overlapped *P*, *Q*, and *R* rotational branches and its full width at half maximum is equal to 35 cm^{-1} . With increasing moment of inertia of the acids, the band of the monomer virtually loses its structure and the half-width of this band decreases to 25 cm^{-1} .

To describe the characteristics of the broad and complex $\nu(\text{OH})$ band of dimers at different temperatures, it is convenient to use the normalized spectral moments: the first spectral moment

$$M_1^* = M_0^{-1} \int S(\nu) \nu d\nu \equiv \nu_0,$$

i.e., the center of gravity of the band ν_0 , and the second spectral moment

$$M_2^* = M_0^{-1} \int S(\nu) (\nu - \nu_0)^2 d\nu,$$

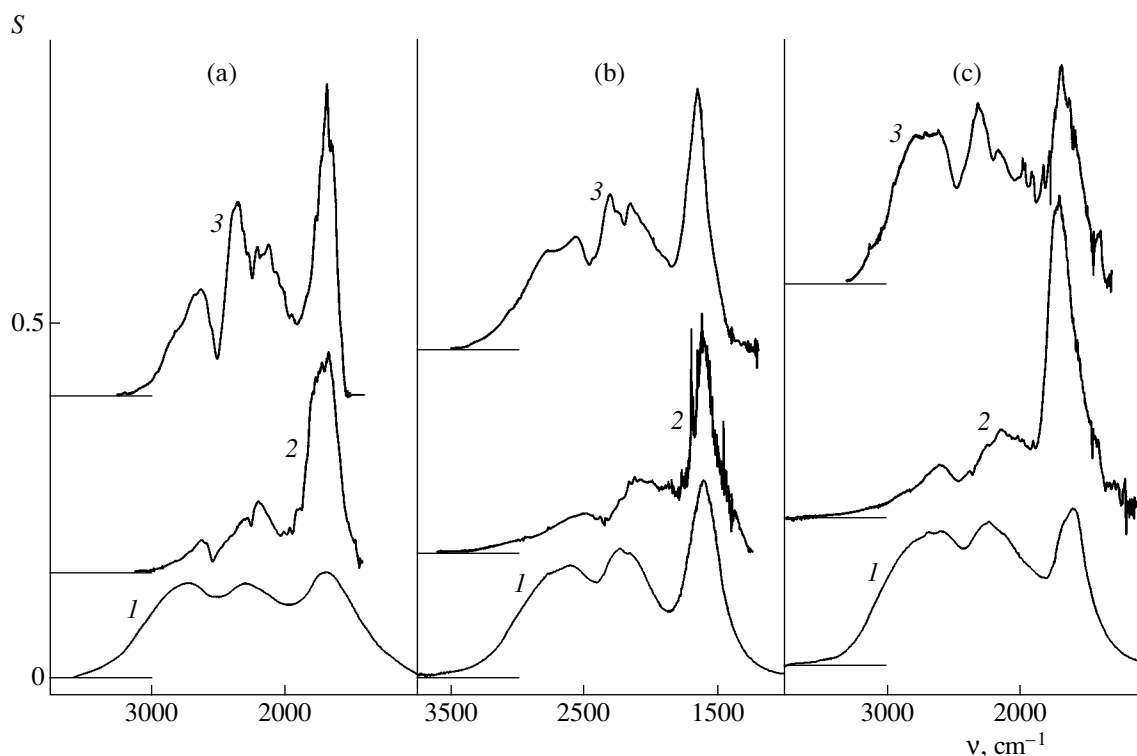


Fig. 2. The $\nu(\text{OH})$ absorption bands of dimers of (a) $(\text{CH}_3)_2\text{POOH}$, (b) $(\text{CH}_2\text{Cl})_2\text{POOH}$, and (c) $(\text{C}_6\text{H}_5)_2\text{POOH}$. Curves: (1) the gas phase at $T =$ (a) 530, (b) 450, and (c) 540 K; (2) the solid phase at $T = 100$ K; and (3) the Ar matrix at $T = 12$ K.

which characterizes the effective half-width of the band $\Delta\nu_{1/2} = 2\sqrt{M_2^*}$. Here, $S(\nu) = D(\nu)/\{v[1 - \exp(-\nu/T)]\}$ is the spectral function, where $D(\nu) = \log I_0/I$ is the optical density and T is the temperature expressed in cm^{-1} , and $M_0 = \int S(\nu)d\nu$. The spectral moments were calculated after separating the bands in the range 4000–1000 cm^{-1} . In this case, the weak wings of the dimer band at $\nu > 3500$ cm^{-1} and $\nu < 1100$ cm^{-1} were extrapolated by exponential functions. The values of ν_0 and

$\Delta\nu_{1/2}$ obtained for all the studied systems in the gas phase, solid samples, and low-temperature matrices are presented in Table 1.

The Shape of the $\nu(\text{OH})$ Band of the $(R_2\text{POOH})_2$ Dimers in the Solid Phase

Figure 1c shows that the absorption spectrum of a solid sample of $(\text{C}_6\text{H}_5)_2\text{POOH}$ deposited in a vacuum onto a CsI window at 80 K and annealed at 300 K is similar to the spectrum of dimers in the gas phase and

Table 1. Center-of-gravity frequencies ν_0 , effective half-widths $\Delta\nu_{1/2}$ (cm^{-1}) of the spectral function $S(\nu)$ of the $\nu(\text{OH})$ absorption band of dimers of phosphinic acids, and dimerization enthalpies ΔH (kcal/mol)

Acid	ΔH , kcal/mol	Gas phase			Crystalline phase			Ar matrix, $T = 12$ K	
		T , K	ν_0	$\Delta\nu_{1/2}$	T , K	ν_0	$\Delta\nu_{1/2}$	ν_0	$\Delta\nu_{1/2}$
$(\text{CH}_3)_2\text{POOH}$	24 ^a	520	2320	1100	200	2030	870	2080	800
		450	2250	1050	100 ^b	1920	750		
$(\text{CH}_2\text{Cl})_2\text{POOH}$	35	475	2150	1050	300	2060	960	2200	960
		435	2130	1020	100 ^b	2050	880		
$(\text{C}_6\text{H}_5)_2\text{POOH}$	50	575	2310	1100	300	1980	870	2250	950
		520	2250	1000	100 ^b	1935	890		

^a [32, 34].

^b After annealing.

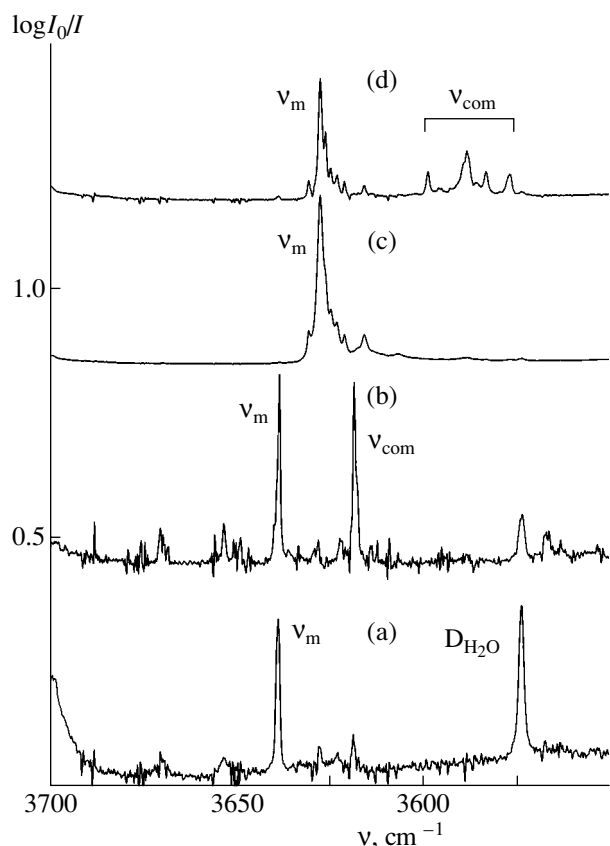


Fig. 3. Absorption spectra of the phosphinic acids R_2POOH in the range of the band $\nu(OH) = \nu_m$ of free molecules in matrices at $T = 12$ K: (a) $(CH_3)_2POOH/Ar$, (b) $(CH_3)_2POOH/Ar/N_2$ ($N_2/Ar = 1/500$), (c) $(CH_2Cl)_2POOH/Ar$, and (d) $(CH_2Cl)_2POOH/Ar/N_2$ ($N_2/Ar = 1/400$). ν_{com} is the $\nu(OH)$ absorption band of the $R_2POOH \cdots N_2$ complex.

that this spectrum also consists of the A, B, and C components. The only difference between these spectra is that the spectrum of the solid film at 100 K shows a marked intensity redistribution: the low-frequency C component of the $\nu(OH)$ band of dimers considerably increases. Such a shape of the absorption band of associates is characteristic of all the acids studied in the crystalline phase (Fig. 2).

The Shape of the $\nu(OH)$ Band of the $(R_2POOH)_2$ Dimers in Low-Temperature Matrices

If the temperature T_0 of a deposited acid is low ($T_0 \approx 20^\circ C$ for $(CH_3)_2POOH$, $T_0 \approx 40^\circ C$ for $(CH_2Cl)_2POOH$, and $T_0 \approx 50^\circ C$ for $(C_6H_5)_2POOH$), the vapor pressure above the solid sample of the acid is low and the dimer concentration is also low; as a result, the absorption spectrum of the R_2POOH/Ar matrix at 12 K exhibits mainly bands of free molecules. The absorption spectrum of free $(C_6H_5)_2POOH$ molecules in an Ar matrix is

shown in Fig. 1e. It exhibits a relatively intense $\nu(OH)$ band of the monomer located at $\nu_m = 3632.6$ cm^{-1} and several bands of internal vibrations at $\nu < 1500$ cm^{-1} . In addition, a number of weak bands of water (3777.3, 3756.7, 3710.6, 1624.0, 1593.2, and 1589.3 cm^{-1}) and CO_2 (2340 cm^{-1}) are also observed in this spectrum. Figure 3 presents the absorption spectra of the phosphinic acids R_2POOH in the range 3700–3500 cm^{-1} . The $\nu(OH)$ bands of the $(CH_3)_2POOH$ and $(CH_2Cl)_2POOH$ monomers in the argon matrix are located at the frequencies $\nu_m = 3638.6$ and 3627.5 cm^{-1} , respectively (Figs. 3a, 3c). In this study, we did not analyze the framework vibrations of the phosphinic acids; however, it should be noted that, in the case of dimethylphosphinic acid, the frequencies of these vibrations for the $(CH_3)_2POOH/Ar$ matrix virtually coincide with those measured previously in [41, 42] for this acid in matrices.

As the effusion temperature T_0 increases, a broad $\nu(OH)$ band of the $(R_2POOH)_2$ dimers appears in the spectra of low-temperature matrices. The intensity of this band, as well as the intensities of the internal vibration bands and the $\nu(OH)$ band of the monomers, increases with T_0 . It is seen from Fig. 1d that the broad band of dimers of $(C_6H_5)_2POOH$ in the argon matrix at 12 K also has the characteristic ABC structure and, on the whole, its shape does not differ from the shape of the dimer bands in the gas phase or in the crystalline films. Moreover, Fig. 4 shows that the bands of dimers of $(CH_3)_2POOH$ (Figs. 4a, 4b) and $(CH_2Cl)_2POOH$ (Figs. 4c, 4d) isolated both in argon and in nitrogen matrices are also similar in shape. In low-temperature nitrogen matrices, apart from the broad $\nu(OH)$ absorption band of dimers, narrow bands of framework vibrations and impurities of H_2O (3727.2 and 1598.4 cm^{-1}) and CO_2 (2348.6 cm^{-1}) are also seen. The broad bands of dimers (Fig. 2) were separated from the experimental spectra using the spectra of free acid molecules.

The Shape of the $\nu(OH)$ Band of Weak $R_2POOH \cdots N_2$ Complexes in Low-Temperature Matrices

At low condensation temperatures, the spectra of argon matrices with a small admixture of nitrogen ($N_2/Ar = 1/200$ – $1/500$) show the $\nu(OH)$ absorption bands of weak $R_2POOH \cdots N_2$ complexes. Figure 3b shows the spectrum of the $(CH_3)_2POOH/Ar/N_2$ matrix in the range of the $\nu(OH)$ absorption band of the monomer. In the spectrum of this mixture, a narrow band appears between the narrow $\nu(OH)$ band of the monomer located at $\nu_m = 3638.6$ cm^{-1} and the band of the H_2O dimers observed at 3573.7 cm^{-1} . The intensity of this band increases with the N_2 concentration, and this band can be attributed to the $\nu(OH)$ vibration of the $(CH_3)_2POOH \cdots N_2$ complex, with its frequency being equal to $\nu_{com} = 3618.6$ cm^{-1} . The low-frequency shift of

the $\nu(\text{OH})$ band $\Delta\nu = \nu_m - \nu_{\text{com}}$ can be used for the estimation of the proton-donating ability of the OH group of the phosphinic acids. In the case of $(\text{CH}_2\text{Cl})_2\text{POOH}$ and $(\text{C}_6\text{H}_5)_2\text{POOH}$, it is necessary to take into account additional features of the spectral manifestations of the formation of the $\text{R}_2\text{POOH}\cdots\text{N}_2$ complexes. First, in the spectra of these acids in argon matrices, the monomer bands have distinct low-frequency wings (Fig. 3c), and, second, the absorption arising due to the formation of nitrogen complexes has a more complicated character than in the case of dimethylphosphinic acid. The spectrum of the $(\text{C}_6\text{H}_5)_2\text{POOH}/\text{Ar}/\text{N}_2$ matrix exhibits a relatively broad band of the $(\text{C}_6\text{H}_5)_2\text{POOH}\cdots\text{N}_2$ complex, whereas, in the spectrum of the system $(\text{CH}_2\text{Cl})_2\text{POOH}/\text{Ar}/\text{N}_2$, in the absorption range of the complex, four components are observed (Fig. 3d), the relative intensities of which virtually do not depend on the nitrogen concentration. Therefore, for the parameter $\Delta\nu$, it is expedient to use the shift of the center of gravity $M_1^*(\text{com})$ of the $\nu(\text{OH})$ band of bound molecules with respect to the center of gravity $M_1^*(\text{m})$ of the $\nu(\text{OH})$ band of free molecules; i.e., $\Delta\nu = M_1^*(\text{m}) - M_1^*(\text{com})$. In the case of $(\text{CH}_3)_2\text{POOH}$ $\nu_m = M_1^*(\text{m})$ and $\nu_{\text{com}} = M_1^*(\text{com})$. Previously, the complicated structure of the $\nu(\text{OH})$ absorption bands of formic acid monomers and $\text{HCOOH}\cdots\text{N}_2$ complexes in Ar matrices was observed in [43]; the low-frequency shift of the $\nu(\text{OH})$ band of this system was observed to be $\sim 12\text{ cm}^{-1}$.

The values of $\Delta\nu$, M_1^* , and $\Delta\nu_{1/2} = 2\sqrt{M_2^*}$ measured for the $\nu(\text{OH})$ absorption bands of the monomers and complexes $\text{R}_2\text{POOH}\cdots\text{N}_2$ of the acids studied are presented in Table 2. It is seen from this table that the shift of the OH band for the $(\text{CH}_3)_2\text{POOH}\cdots\text{N}_2$ complex is equal to 20.3 cm^{-1} . In the case of the chlorine-substituted $(\text{CH}_2\text{Cl})_2\text{POOH}$ acid, this shift increases to 35 cm^{-1} , and, for the $(\text{C}_6\text{H}_5)_2\text{POOH}\cdots\text{N}_2$ complex, it decreases to 23 cm^{-1} . The proton-donating ability of the R_2POOH acids should vary in the same way. The energy of the cyclic dimer with two hydrogen bonds $-\text{OH}\cdots\text{O}=\text{P}-$, which depends both on the proton-

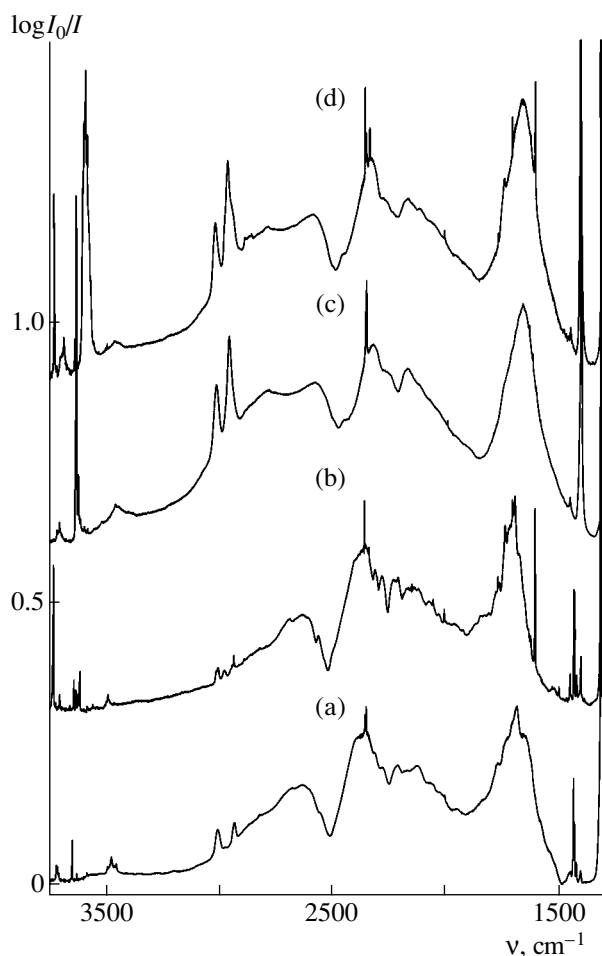


Fig. 4. Absorption spectra of (a, b) $(\text{CH}_3)_2\text{POOH}$ and (c, d) $(\text{CH}_2\text{Cl})_2\text{POOH}$ in (a, c) Ar and (b, d) N_2 matrices at $T = 12\text{ K}$.

donating ability of the OH group and on the proton-accepting ability of the $\text{P}=\text{O}$ group, successively increases from 25 to 50 kcal/mol . From comparing the low-frequency shifts of the $\nu(\text{OH})$ band of the $\text{R}_2\text{POOH}\cdots\text{N}_2$ complexes and the shifts of the $\nu(\text{AH})$ band of the $\text{AH}\cdots\text{N}_2$ complexes, which for the strong proton donors $\text{AH}=\text{FH}$ and *trans*-HONO are equal,

Table 2. Center-of-gravity frequencies and the effective band widths $\Delta\nu_{1/2}$ (cm^{-1}) of the $\nu(\text{OH})$ absorption bands of the monomers of R_2POOH ($M_1^*(\text{m})$) and their nitrogen complexes $\text{R}_2\text{POOH}\cdots\text{N}_2$ ($M_1^*(\text{com})$) in Ar matrices at 12 K $\Delta\nu_{1/2}$, $\Delta\nu = M_1^*(\text{m}) - M_1^*(\text{com})$

Acid	Monomer		Complex		$\Delta\nu$
	$M_1^*(\text{m})$	$\Delta\nu_{1/2}$	$M_1^*(\text{com})$	$\Delta\nu_{1/2}$	
$(\text{CH}_3)_2\text{POOH}$	3638.8(3)	1.6(7)	3618.5(2)	2.8(3)	20.3(5)
$(\text{CH}_2\text{Cl})_2\text{POOH}$	3624.8(7)	9(2)	3589(1)	10(2)	35(2)
$(\text{C}_6\text{H}_5)_2\text{POOH}$	3630.3(8)	13.5(9)	3607.5(3)	18(4)	23(1)

respectively, to 43.2 cm^{-1} [44] and 10.4 cm^{-1} [45], we can conclude that the phosphinic acids belong to the strongest proton donors.

DISCUSSION OF RESULTS AND MODEL CALCULATIONS OF THE BAND CONTOUR

For all the acids under investigation, the spectral functions $S(\nu)$ of the $\nu(\text{OH})$ absorption bands of the dimers of the acid molecules separated from the experimental spectra of these acids in argon matrices at 12 K, in the gas phase at $T = 460\text{--}520\text{ K}$, and in crystalline films at 100 K are presented in Fig. 2. The spectral moments of these bands are summarized in Table 1. The results obtained for dimers with different energies in the wide temperature range 12–600 K allow us to formulate some considerations regarding the formation of the absorption bands of strongly hydrogen-bonded systems.

1. Upon formation of the $(\text{R}_2\text{POOH})_2$ dimers of all the phosphinic acids in all the systems and in the entire temperature range under consideration, broad $\nu(\text{OH})$ absorption bands (one could say anomalously broad: $\Delta\nu_{1/2} \sim 1000\text{ cm}^{-1}$) arise, the centers of gravity of which are shifted toward the low-frequency range by $1300\text{--}1500\text{ cm}^{-1}$. It is clear that such considerable temperature shifts of the $\nu(\text{OH})$ band are characteristic of very strong hydrogen bonds. This is consistent with the values of the dimerization energies of R_2POOH , which were determined in [30, 32] to fall in the range 25–50 kcal/mol (Table 1). In this energy range, the values of the low-frequency shifts virtually do not vary with increasing strength of the dimers.

2. For all the acids under consideration, the broad dimer bands have the so-called ABC structure, which was observed first in the spectra of strongly hydrogen-bonded crystals [38–40]. For the dimers studied, we were able to observe the ABC structure both in the gas phase and in inert low-temperature matrices. Commonly, the appearance of valleys (windows) in the contour of the broad absorption band of complexes is attributed to Fermi resonance between the first excited state of the $\nu(\text{OH})$ mode and the doubly degenerate states of the bending vibrations of the hydroxyl group $2\gamma\text{OH}$ and $2\delta\text{OH}$ [40]; i.e., the frequencies of the minima observed can be associated with the frequencies of overtones of bending vibrations. Note that, on the whole, the positions of the maxima and minima of the observed ABC structure depend weakly on the type of the acid and the experimental conditions. The high-frequency minima between the A and B components are associated with the $2\delta\text{OH}$ transitions and, in the gas phase, are observed at 2475 , 2415 , and 2400 cm^{-1} for $(\text{CH}_3)_2\text{POOH}$, $(\text{CH}_2\text{Cl})_2\text{POOH}$, and $(\text{C}_6\text{H}_5)_2\text{POOH}$, respectively. The low-frequency minima between the B and C components, related to the $2\gamma\text{OH}$ transitions, are located at 1905 , 1850 , and 1855 cm^{-1} , respectively.

The quantitative analysis of the Fermi resonance in these systems requires knowledge of the exact frequencies of transitions in the range of framework vibrations of monomers and dimers of the phosphinic acids under consideration. A reliable interpretation of their spectra in this frequency range should be based on ab initio calculations of anharmonic vibrational problems. To date, the vibrational spectra of the monomer and the dimer of $(\text{CH}_3)_2\text{POOH}$ [46] and the spectrum of the monomer of its acid [42] have been calculated in the harmonic approximation. In the first of these two studies, an insufficiently complete set of atomic orbitals was used, and, in the second investigation, the potential surface was determined semiempirically. It seems that this may be the reason for the considerable discrepancies in the interpretation of the vibrational modes and calculated frequencies even in the case of the monomer.

3. The intensity distribution between the A, B, and C components of the absorption band of a dimer depends primarily on the phase state of a substance. The band shape depends only insignificantly on the type of the phosphinic acid under study. Radical changes are observed on passage from the gas phase to polycrystalline films. As is seen from Fig. 2 (curves 2), the intensity of the A, B, and C components in the spectra of the annealed solid films is redistributed in favor of the C component, with the shapes of the $\nu(\text{OH})$ absorption bands of the dimers of all the acids being practically identical. The effective half-widths of the bands in the spectra of solid films decrease as compared to the gases. It is obvious that the intensity redistribution in favor of the low-frequency component in the spectra of crystals leads to a low-frequency shift of the center of gravity of the absorption band (Table 1). The spectra of the low-temperature matrices $(\text{CH}_2\text{Cl})_2\text{POOH}/\text{Ar}$ and $(\text{C}_6\text{H}_5)_2\text{POOH}/\text{Ar}$ differ little from the high-temperature spectra in the gas phase; for the $(\text{CH}_3)_2\text{POOH}/\text{Ar}$ matrix, the absorption band of the dimer occupies a position intermediate between its positions in the spectra of the gas phase and the solid film.

We can attempt to relate the observed differences in the band shapes of the phosphinic acids in the gas and crystalline phases to different structures of the associates in these systems. According to x-ray and neutron diffraction data [47–49], in the crystalline phase, the molecules of phosphoric acids form helical chains stabilized by hydrogen bonds $\text{O}\cdots\text{H}\cdots\text{O}=\text{P}$. The distances between oxygen atoms $\text{O}\cdots\text{O}=\text{P}$, which characterize the bond strength, were measured; in particular, it was found that, in the $(\text{CH}_3)_2\text{POOH}$ crystal, $R_{\text{O}\cdots\text{O}} = 2.48\text{ \AA}$. Since [30], it has been assumed that, in the gas phase, these molecules form cyclic dimers with two hydrogen bonds. Experimentally, this assumption was confirmed for dimethylphosphinic acid by the method of gas electronography [50, 51]. It was also shown in these studies that the distance between the oxygen atoms in the cyclic dimer is equal to $R_{\text{O}\cdots\text{O}} = 2.69\text{ \AA}$; i.e., it is greater than in the crystal. Therefore, one may think

that the hydrogen bonds in the crystal are stronger and that it is this fact that causes changes in the shape of the absorption band. However, the measurement results for the gas phase show that the increase in the energy of the dimers (due to the formation of two hydrogen bonds) to 24 kcal/mol for $(\text{CH}_3)_2\text{POOH}$, to 35 kcal/mol for $(\text{CH}_2\text{Cl})_2\text{POOH}$, and to 50 kcal/mol for $(\text{C}_6\text{H}_5)_2\text{POOH}$ (Fig. 2; Table 1) has no significant effect on the position or the shape of the $\nu(\text{OH})$ band of the hydrogen-bonded molecules. Therefore, we are led to accept that the observed changes in the shape of this band are primarily related to changes in the structure of associates in polycrystalline films. The similarity between the spectra measured in the gas phase and in the low-temperature matrices follows from the fact that the low-temperature matrices are obtained by condensation of gaseous mixtures $\text{R}_2\text{POOH}/\text{M}$ at low temperatures. Note that the notion of a correlation between the length of a hydrogen bridge and the energy of the corresponding hydrogen bond was mainly developed on the basis of measurements of $R_{\text{A...B}}$ in crystals, for which the energy cannot be directly measured.

4. As follows from our results, no radical changes in the spectral characteristics of the $\nu(\text{OH})$ absorption band of dimers occur in the temperature range 600–12 K. Clearly, the spectral characteristics of the broad band of dimers of these acids do exhibit some weak temperature dependence. However, it takes place only for the given phase state of the substance. Thus, in the gas phase, one can note a small decrease in the effective half-width $\Delta\nu_{1/2}$ and an increase in the intensity of the C component, which result in a low-frequency shift of the center-of-gravity frequency ν_0 with decreasing temperature. In the crystalline state, the intensity of the C component also increases with decreasing temperature and, consequently, the frequency ν_0 decreases [32, 33]. At low temperatures, the band structure becomes more distinct (see also Fig. 4), while the positions of the absorption minima change little.

Our results allow us to state that, for all the phosphinic acids studied, irrespective of their type, the $\nu(\text{OH})$ absorption bands of their dimers observed in the IR spectra are similar in structure and are very broad ($\Delta\nu_{1/2} \sim 1000 \text{ cm}^{-1}$). This means that the mechanism of formation of these bands should, first of all, involve the participation of the fragment $-\text{POOH}$, responsible for the formation of the hydrogen bond. Insignificant changes in the shape of the dimer band observed upon passage from cyclic complexes in the gas phase to helical chains stabilized by hydrogen bonds in the crystalline state allow us to believe that the interaction of the two intermolecular bonds $\text{O}-\text{H...O}=\text{P}$ in a cyclic complex does not play a determining role in the formation of the broad absorption band. Finally, the weak temperature dependence of the width of the dimer band and of its ABC structure in the temperature range 12–600 K means that, upon formation of strong hydrogen-bonded complexes, a number of temperature-independent

vibrational transitions appear in the range 3500–1500 cm^{-1} , which account for the structure and considerable width of this band.

Numerous studies have attempted to account for the observed width and structure of the $\nu(\text{OH})$ absorption band of dimers of carboxylic acids [52–54]. Of special interest in this respect is [11], in which the frequencies and intensities of the vibrational transitions arising due to resonance interactions between the first excited state of the $\nu(\text{OH})$ mode of dimers and doubly excited or combination states of the stretching $\text{C}=\text{O}$ and $\text{C}-\text{O}$ and bending OH vibrations were calculated. These calculations made it possible to explain the structure of the absorption band of the $(\text{CH}_3\text{COOH})_2$ dimer. By analogy, one can suggest the occurrence of similar interactions in the case of the $(\text{R}_2\text{POOH})_2$ dimer; however, a rigorous analysis of the structure of the anomalously broad $\nu(\text{OH})$ band of the phosphinic acid dimers requires the solution of an anharmonic vibrational problem. There is little doubt that the interactions between the $\nu(\text{OH})$ vibration and the low-frequency intermolecular vibrations of the dimer should play an important role in the formation of this band. The remaining part of our study is devoted to the analysis of the possible contribution from this mechanism.

5. Let us consider the basic features of the absorption that arises due to the interactions between the band $\nu(\text{AH}) = \nu(\text{OH}) = \nu_1$ and the intermolecular low-frequency vibrations ν_k of a complex (this mechanism is involved in the formation of the absorption bands of practically all molecular complexes in the gas phase). A superposition of the fundamental ν_1 transition and hot and combination (in particular, sum and difference) transitions involving the participation of low-frequency vibrations results in the formation of the absorption band of a complex. To calculate this band, one needs to know the frequencies and intensities of the transitions, as well as the rotational structure of individual vibrational bands. For complexes with a large moment of inertia, each rotational-vibrational band can be approximated by a simple Lorentzian (or Gaussian) contour.

The intensities of the combination transitions can be estimated in terms of a simple anharmonic model [4, 55], which assumes that, upon excitation of the ν_1 stretching vibration, the shift of the potential energy minimum of the k th low-frequency vibration is proportional to the parameter b_k , determined by the quantum-mechanical amplitude of the low-frequency vibration. For example, for the ν_3 stretching low-frequency vibration, the parameter $b_3 = \alpha_{113}/\omega_3$, where ω_3 is the harmonic frequency of the low-frequency vibration and α_{113} is the cubic force constant in a power series expansion of the potential energy in terms of the dimensionless normal coordinates. In this case, the intensities of the transitions $(\nu_1 = 0, \nu_3) \rightarrow (1, \nu'_3)$, where ν_3 and ν'_3 are the vibrational quantum numbers of the ν_3 mode

in the ground state and in the excited v_1 state, are determined by integrals of the Franck–Condon type.

In the general case, the vibrational term of a complex $E(v_1, v_2, \dots, v_7)$, where v_1 is the quantum number of the v_1 vibrational mode and v_2 – v_7 are the quantum numbers of the low-frequency intermolecular vibrations v_k (in the general case, six new vibrational degrees of freedom appear upon formation of a dimer), can be represented in the form

$$E(v_1, v_2, \dots, v_7) = \omega_1(v_1 + 1/2) + x_{11}(v_1 + 1/2)^2 + \sum_{k=2}^7 \omega_k(v_k + 1/2) + \frac{1}{2} \sum_{k=1}^7 x_{km}(v_k + 1/2)(v_m + 1/2). \quad (1)$$

Here, ω_1 and ω_k are the harmonic frequencies of the vibrations v_1 and v_k , respectively, while x_{11} , x_{1k} , and x_{km} are the anharmonicity constants. The $v(\text{OH})$ band of the complex is a superposition of the vibrational–rotational bands of transitions from the level $E(v_1 = 0, v_2, \dots, v_7)$ to the level $E(1, v'_2, \dots, v'_7)$. The vibrational frequencies of these transitions are given by

$$v_{0, v_2, \dots, v_7}^{1, v'_2, \dots, v'_7} = E(1, v'_2, \dots, v'_7) - E(0, v_2, \dots, v_7) \quad (2)$$

and the transition intensities are expressed as

$$I_{0, v_2, \dots, v_7}^{1, v'_2, \dots, v'_7} = A \frac{1}{Z(T)} v_{0, v_2, \dots, v_7}^{1, v'_2, \dots, v'_7} (n_{0, v_2, \dots, v_7} - n_{1, v'_2, \dots, v'_7}) |P_{0, v_2, \dots, v_7}^{1, v'_2, \dots, v'_7}|^2. \quad (3)$$

In (3), A is a constant;

$$P_{0, v_2, \dots, v_7}^{1, v'_2, \dots, v'_7} = \langle \psi_{1, v'_2, \dots, v'_7} | P | \psi_{0, v_2, \dots, v_7} \rangle \quad (4)$$

is the matrix element of the dipole transition between the corresponding vibrational levels;

$$n_{v_1, v_2, \dots, v_7} \propto \exp\left(-\frac{E_{v_1, v_2, \dots, v_7}}{kT}\right)$$

is the population of a level; $Z(T)$ is the statistical sum; and T is the temperature. The formation of the absorption band involves the participation of the fundamental transition ($v_1 = 0, v_2 = 0, \dots, v_7 = 0$) \rightarrow ($1, 0, \dots, 0$), as well as sum ($0, 0, \dots, 0$) \rightarrow ($1, v'_2, \dots, v'_7$), difference ($0, v_2, \dots, v_7$) \rightarrow ($1, 0, \dots, 0$), combination ($v_1 = 0, \dots, v_k = 0, v_m \neq 0, \dots$) \rightarrow ($1, \dots, v'_k \neq 0, v'_m = 0, \dots$), and hot transitions.

Dipole transition matrix elements (4) were calculated using the expansion of the dipole moment function in terms of the dimensionless vibrational coordinates q_k [55],

$$P = P_0 + P'_1 q_1 + \sum_{k=2}^7 P'_k q_k + (1/2) P''_{11} q_1^2 + \sum_{k=2}^7 P''_{1k} q_1 q_k + (1/2) \sum_{k,m=2}^7 P''_{km} q_k q_m + \dots \quad (5)$$

As wave functions $\psi_{v_1 v_2 \dots v_7}$ of the given vibrational state, products of the harmonic oscillator wave functions $\phi_{v_k}(q_k)$ with the corresponding harmonic frequencies were used. In this case, we assumed that, upon excitation of the vibration $v_1 = v(\text{OH})$, the position of the minimum of the potential well of the low-frequency vibration v_k changes by a dimensionless quantity $b_k(v_1 + 1/2)$; i.e.,

$$\psi_{v_1 v_2 \dots v_7} = \phi_{v_1}(q_1) \prod_{k=2}^7 \phi_{v_k}(q_k + b_k(v_1 + 1/2)). \quad (6)$$

In this approximation, from (4)–(6), we obtain

$$P_{0, v_2, \dots, v_7}^{1, v'_2, \dots, v'_7} = \frac{P'_1}{\sqrt{2}} \prod_{k=2}^7 D_{v_k, v'_k} + \sum_{k=2}^7 \frac{P''_{1k}}{\sqrt{2}} \left[\left(\sqrt{\frac{v_k+1}{2}} D_{v_k+1, v'_k} + \sqrt{\frac{v_k}{2}} D_{v_k-1, v'_k} \right) \prod_{\substack{m=2, \\ m \neq k}}^7 D_{v_m, v'_m} \right]. \quad (7)$$

Here, P'_1 and P''_{1k} are the derivatives of the dipole moment function with respect to the corresponding dimensionless normal coordinates and D_{v_k, v'_k} are the Franck–Condon factors:

$$D_{v_k, v'_k} = \int \phi_{v'_k}^*(q_k + b_k) \phi_{v_k}(q_k) dq = (-1)^{v_k + v'_k} D_{v'_k, v_k}.$$

At $v'_k \geq v_k$, we have

$$D_{v_k, v'_k} = \exp(-b_k^2/4) \sqrt{v_k! v'_k!} \times \sum_{m=0}^{v'_k} (-1)^m \left(\frac{b_k}{\sqrt{2}} \right)^{2m + v'_k - v_k} \frac{1}{m! (v_k - m)! (v'_k - v_k + m)!}. \quad (8)$$

Applicability of the Model to the Description of the Broad $\nu(\text{OH})$ Absorption Band

In order to apply the proposed model to the calculation of the absorption band contour, independent experimental and calculational data on the frequencies ω_1 and ω_k of a strongly hydrogen-bonded complex, as well as on the anharmonicity constants x_{km} , the parameters b_k , and the characteristics of the corresponding vibrational–rotational contours, should be available. Unfortunately, the literature does not contain data on the interaction potentials for the phosphinic acid dimers, which are necessary for the calculation of the quantities x_{km} and b_k , or the derivatives of the dipole moment with respect to the normal coordinates. Therefore, at this stage of our investigation, it is worthwhile to consider a simpler problem and to estimate the possible contribution from the mechanism under study to the formation of the band contour of the strong H bond. To simplify the problem, we can assume that, for the low-frequency vibrations, $x_{km} = 0$ ($k \neq 1, k \neq m$) and $P''_{1k} = 0$; i.e., the electro-optical anharmonicity is neglected. Accordingly, expressions (1) and (3) will become simpler and, instead of (7), we will obtain

$$P_{0, \nu_2, \dots, \nu_7}^{1, \nu'_2, \dots, \nu'_7} = \frac{P_1'}{\sqrt{2}} \prod_{k=2}^7 D_{\nu_k, \nu'_k}. \quad (9)$$

The integrated intensity of the $\nu(\text{OH})$ band is equal to the sum of the intensities of all the transitions:

$$I_{\nu(\text{OH})} = \sum_{\substack{\nu'_2, \dots, \nu'_7 \\ \nu_2, \dots, \nu_7}} I_{0, \nu_2, \dots, \nu_7}^{1, \nu'_2, \dots, \nu'_7}. \quad (10)$$

From (3) and (9), it follows that both the intensities of the individual transitions and the integrated intensity of the entire band are proportional to $(P_1')^2$; therefore, the intensities were calculated in terms of the relative units $\hat{I} = (I/A)(P_1')^2$.

We estimated the absorption band characteristics for the dimers of $(\text{CH}_3)_2\text{POOH}$ since it is this acid for which the ab initio calculations of the vibrational frequencies of monomers and dimers were carried out [46, 51]. For this purpose, the following values of the calculated harmonic frequencies were used [46]: $\omega_1 = 2893$, $\omega_2 = 394$, $\omega_3 = 368$, $\omega_4 = 243$, and $\omega_5 = 204 \text{ cm}^{-1}$. Preliminary calculations showed that taking into account the low-frequency vibrations with $\omega_6 = 26$ and $\omega_7 = 23 \text{ cm}^{-1}$ has virtually no effect on the effective width of the dimer band. The parameters x_{kk} , x_{1k} , and b_k were determined from comparison of the experimental and calculated contours using nonlinear multidimensional optimization under the assumption that $|x_{kk}| < 0.2\omega_k$ and $0 < x_{1k} < 0.2\omega_k$. As a rotational contour, we used a Lorentz contour with a half-width of $30\text{--}40 \text{ cm}^{-1}$.

As was noted above, the ABC structure observed can be associated both with the Evans windows in the inhomogeneously broadened band [56] and with the resonance interaction between the first excited state of the $\nu(\text{OH})$ dimer mode and the doubly excited or combination states of the stretching $\text{P}=\text{O}$ and $\text{P}-\text{O}$ and bending OH vibrations. For this reason, it was worthwhile to clarify whether it is possible to describe the formation of the entire broad dimer band ($\Delta\nu_{1/2} \sim 1000 \text{ cm}^{-1}$) and one of the components of the ABC structure within the framework of the model under consideration.

Here, we will consider three variants of comparison of the calculation results with experiment: (I) comparison of the integral characteristics (the spectral moments) of the $\nu(\text{OH})$ band in the range $3500\text{--}1000 \text{ cm}^{-1}$ for different temperatures, (II) comparison of the experimental and calculated band contours in the range $3500\text{--}1000 \text{ cm}^{-1}$, and (III) comparison of the calculated band contours with the contours of the subbands obtained from the separation of the broad $\nu(\text{OH})$ band into several components.

Variant I. In fitting the parameters x_{kk} , x_{1k} , and b_k , we minimized the sum of the squares of the differences of the effective $\Delta\nu_{1/2} = 2\sqrt{M_2^*}$, experimental $\Delta\nu_{1/2}^{\text{exp}}$, and calculated $\Delta\nu_{1/2}^{\text{calc}}$ half-widths of the $\nu(\text{OH})$ absorption band

$$\Phi_1 = [\Delta\nu_{1/2}^{\text{exp}}(T_1) - \Delta\nu_{1/2}^{\text{calc}}(T_1)]^2 + [\Delta\nu_{1/2}^{\text{exp}}(T_2) - \Delta\nu_{1/2}^{\text{calc}}(T_2)]^2$$

found at the temperatures $T_1 = 12 \text{ K}$ and $T_2 = 460 \text{ K}$. In the fitting process, the frequency ω_1 , on the value of which the center-of-gravity frequency of the entire ν_0 band depends substantially, was also varied. A satisfactory agreement between the calculation and experiment was obtained for the following parameters: $x_{22} = -65$, $x_{33} = -61$, $x_{44} = 31$, $x_{55} = -22 \text{ cm}^{-1}$, $x_{12} = 69$, $x_{13} = 65$, $x_{14} = 11$, $x_{15} = 40 \text{ cm}^{-1}$, $b_2 = 0.9$, $b_3 = 1.6$, $b_4 = 0.7$, $b_5 = 1.6$, and $\omega_1 = 2015 \text{ cm}^{-1}$. On the whole, this set of the parameters seems to be reasonable; however, it should be stressed that the parameters b_3 and b_5 are overestimated. Using the intermolecular vibrations with the frequencies $\omega_2 = 394 \text{ cm}^{-1}$ and $\omega_3 = 368 \text{ cm}^{-1}$ as an example, one can gain some idea of the intensities of the sum and difference transitions at $T = 460 \text{ K}$ (the values of \hat{I}) are given in the parentheses: $\nu_{0,0,0,0,0}^{1,0,0,0,0} = 1869 \text{ cm}^{-1}$ (2.24), $\nu_{0,0,0,0,0}^{1,1,0,0,0} = 2240 \text{ cm}^{-1}$ (1.23), $\nu_{0,1,0,0,0}^{1,0,0,0,0} = 1570 \text{ cm}^{-1}$ (0.28), $\nu_{0,0,0,0,0}^{1,2,0,0,0} = 2481 \text{ cm}^{-1}$ (0.30), $\nu_{0,2,0,0,0}^{1,0,0,0,0} = 1401 \text{ cm}^{-1}$ (0.03), and $\nu_{0,0,0,0,0}^{1,3,0,0,0} = 2591 \text{ cm}^{-1}$ (0.04). However, although the calculated and experimental half-widths agree well with each other in a wide

temperature range, the calculated contour is far from the experimental one.

Variant II. In this case, we attempted to describe the shape of the contour of the broad $\nu(\text{OH})$ band with the ABC structure at 530 K. In fitting the parameters x_{kk} , x_{1k} , b_k , and the frequency ω_1 , we minimized the function

$$\Phi_2 = \int \left(\frac{D_{\text{exp}}(\nu)}{\int D_{\text{exp}}(\nu) d\nu} - \frac{D_{\text{calc}}(\nu)}{\int D_{\text{calc}}(\nu) d\nu} \right)^2 d\nu,$$

where $D_{\text{exp}}(\nu)$ and $D_{\text{calc}}(\nu)$ are the current optical densities of the experimental and calculated spectra, respectively. The broad absorption band, which describes qualitatively the observed intensity distribution ($\Phi_2 = 2.5 \times 10^{-5}$) in the range 3500–1000 cm^{-1} , was obtained at $x_{22} = -11$, $x_{33} = -14$, $x_{44} = -9$, $x_{55} = -17$ cm^{-1} , $x_{12} = 2.5$, $x_{13} = 0$, $x_{14} = 19$, $x_{15} = 22$ cm^{-1} , $b_2 = 1.2$, $b_3 = 1.1$, $b_4 = 0.9$, $b_5 = 1.2$, $\omega_1 = 2083$ cm^{-1} , and $x_{11} = -200$ cm^{-1} . This set of the parameters enables only qualitative description of the temperature behavior of the spectrum in the range 500–12 K.

Variant III. The $\nu(\text{OH})$ absorption band of dimers of dimethylphosphinic acid in the gas phase at $T = 460$ K was separated into three subbands with close half-widths, $\Delta\nu_{1/2} \sim 600$ cm^{-1} , and maxima corresponding to the maxima of the ABC structure located at $\nu_A = 2740$ cm^{-1} , $\nu_B = 2240$ cm^{-1} , and $\nu_C = 1685$ cm^{-1} , respectively. As an example, we calculated the contour of the A subband varying the parameters ω_A , x_{kk} , x_{1k} , and b_k in the frequency range 3500–1750 cm^{-1} . The frequency ω_A can be considered to correspond to the harmonic frequency of the transition occurring due to the resonance interaction in the $-\text{POOH}$ group. In the course of the nonlinear optimization, the rms deviation Φ_2 between the calculated and experimental contours, the integrated intensity of which is equal to unity, was minimized. As a result, a reasonable set of the parameters was obtained ($\Phi_2 = 1.6 \times 10^{-6}$): $\omega_A = 2490$ cm^{-1} , $x_{AA} = 3$, $x_{22} = -49$, $x_{33} = -46$, $x_{44} = -30$, $x_{55} = -25$, $x_{A2} = 31$, $x_{A3} = 30$, $x_{A4} = 14$, $x_{A5} = 5$ cm^{-1} , $b_2 = 0.45$, $b_3 = 0.55$, $b_4 = 1.4$, and $b_5 = 1.13$. It is obvious that, due to fairly large (for the strong hydrogen bond) parameters $b_k \geq 1$ [55], an appreciable number of combination transitions are involved in the formation of the spectrum. Thus, for $\omega_4 = 243$ cm^{-1} ($b_4 = 1.4$), the following transitions contribute to the spectrum (the values of \hat{I}) are given in the parentheses: $\nu_{0,0,0,0,0}^{1,0,0,0,0} = 2538$ cm^{-1} (5.7), $\nu_{0,0,0,0,0}^{1,0,0,1,0} = 2741$ cm^{-1} (6.0), $\nu_{0,0,0,1,0}^{1,0,0,0,0} = 2348$ cm^{-1} (3.1), $\nu_{0,0,0,0,0}^{1,0,0,2,0} = 2884$ cm^{-1} (3.1), $\nu_{0,0,0,2,0}^{1,0,0,0,0} = 2220$ cm^{-1} (1.0), $\nu_{0,0,0,0,0}^{1,0,0,3,0} = 2966$ cm^{-1} (1.0), and $\nu_{0,0,0,3,0}^{1,0,0,0,0} = 2152$ cm^{-1} (0.3). For smaller b_k , the intensity of the combination transitions

decreases markedly. Thus, for $b_2 = 0.45$, a noticeable contribution is made only by the transition $\nu_{0,0,0,0,0}^{1,1,0,0,0} = 2859$ cm^{-1} ($\hat{I} = 0.97$). This analysis shows that, in the case of variant III, the shape of the separated subband can be described with the use of the set of plausible parameters. Generally, in our opinion, anharmonic interactions between high- and low-frequency vibrations contribute considerably to the formation of the absorption band of a strong hydrogen bond. Clearly, for the comparison between the calculated and the experimental contours to be unambiguous, one should solve an ab initio anharmonic problem for the phosphinic acid dimer and determine the quantities ω_k , x_{kk} , and x_{1k} . Then it is necessary to study the nature of the vibrational structure of the band as a whole.

CONCLUSIONS

Our investigation of the $\nu(\text{OH})$ absorption band of strongly hydrogen-bonded dimers formed by phosphinic acids R_2POOH in the gas and solid phases and in low-temperature matrices shows that these bands for all the acids, irrespective of their type, phase state, and temperature, are broad ($\Delta\nu_{1/2} \sim 1000$ cm^{-1}) and similar in shape, exhibiting a characteristic ABC structure. It is demonstrated that the formation of such an anomalously broad absorption band is primarily associated with the $-\text{POOH}$ fragment, involved in the hydrogen bonding; the interaction between the two intermolecular bonds $\text{O}-\text{H} \cdots \text{O}=\text{P}$ in a cyclic complex plays virtually no role in this mechanism of hydrogen bond formation. Finally, the weak temperature dependence of the width and the structure of the dimer band in the range 12–600 K means that, upon formation of strongly hydrogen-bonded complexes, a number of vibrational transitions appear in the frequency range 3500–1000 cm^{-1} , whose intensity weakly depends on the temperature. All such transitions determine the structure and the half-width of the absorption band.

Within the framework of a model that takes into account anharmonic interactions between the $\nu(\text{OH})$ mode and the low-frequency intermolecular vibrations ν_k of the complex, the intensities of the combination transitions $\nu(\text{OH}) \pm m\nu_k$ are estimated. It is shown that, using a set of reasonable spectral parameters, one can describe the main features (first of all, the effective half-width) of the observed dimer absorption band, which, apart from the fundamental transition, is formed as a result of superposition of hot and combination transitions.

ACKNOWLEDGMENTS

This study was supported by the Russian Foundation for Basic Research, project no. 03-03-32272. The support of the Faculty of Chemistry of the University of Wrocław is gratefully acknowledged.

REFERENCES

1. C. Sandorfy, *Hydrogen Bonds*, Ed. by P. Schuster (Akademie, Berlin, 1984), pp. 41–84.
2. J. Lascombe and J. C. Lassegues, *Mol. Phys.* **40**, 969 (1980).
3. A. C. Legon and D. J. Millen, *Chem. Rev.* **86**, 635 (1986).
4. D. N. Shchepkin, *J. Mol. Struct.* **156**, 303 (1987).
5. K. G. Tokhadze and S. S. Utkina, *Chem. Phys.* **294**, 45 (2003).
6. V. P. Bulychiev, E. I. Gromova, and K. G. Tokhadze, *Opt. Spektrosk.* **96** (5), 843 (2004) [*Opt. Spectrosc.* **96**, 774 (2004)].
7. G. V. Yikhnevich, E. G. Tarakanova, V. D. Maïorov, and N. B. Librovich, *Usp. Khim.* **64**, 963 (1995).
8. D. Chamma, *J. Mol. Struct.* **552**, 187 (2000).
9. G. Zundel, *Adv. Chem. Phys.* **111**, 1 (2000).
10. O. Henry-Rousseau, *Adv. Chem. Phys.* **121**, 241 (2002).
11. C. Emmeluth, M. A. Suhm, and D. Luckhaus, *J. Chem. Phys.* **118**, 2242 (2003).
12. V. E. Borisenko, G. S. Denisov, E. V. Maximov, *et al.*, *Spectrosc. Lett.* **26**, 1139 (1993).
13. J. P. Castaneda, G. S. Denisov, S. Y. Kuchero, *et al.*, *J. Mol. Struct.* **660** (1–3), 25 (2003).
14. S. E. Odinov, V. P. Glazunov, and A. A. Nabiullin, *J. Chem. Soc., Faraday Trans. 2* **80**, 899 (1984).
15. V. A. Ozeryanski, A. F. Pozharskii, T. Glowiak, *et al.*, *J. Mol. Struct.* **607** (1), 1 (2002).
16. M. Rozenberg, A. Loewenschuss, and Y. Marcus, *Phys. Chem. Chem. Phys.* **2** (12), 2699 (2000).
17. Yu. Ya. Efimov, *Izv. Ross. Akad. Nauk, Ser. Khim.* **52** (1), 261 (2003).
18. A. V. Iogansen, *Spectrochim. Acta A* **55**, 1585 (1999).
19. Th. Zeegers-Huyskens, in *Intermolecular Forces. An Introduction to Modern Methods and Results*, Ed. by P. L. Huyskens, W. A. P. Luck, and T. Zeegers-Huyskens (Springer, Berlin, 1991), pp. 123–155.
20. A. J. Barnes, T. R. Beech, and Z. Mielke, *J. Chem. Soc., Faraday Trans. 2* **80**, 455 (1984).
21. J. E. Del Bene and M. J. T. Jordan, *J. Chem. Phys.* **108**, 3205 (1998).
22. L. Andrews, X. Wang, and Z. Mielke, *J. Phys. Chem. A* **105**, 6054 (2001).
23. L. Andrews and X. Wang, *J. Phys. Chem. A* **105**, 7541 (2001).
24. J. Emsley, *Chem. Soc. Rev.* **9**, 91 (1980).
25. D. Hadzi and B. Orel, *J. Mol. Struct.* **18**, 227 (1973).
26. D. Hadzi, *Pure Appl. Chem.* **11**, 435 (1965).
27. J. A. Walmsley, *J. Phys. Chem.* **88**, 1226 (1984).
28. S. Detoni and D. Hadzi, *Spectrochim. Acta* **20**, 949 (1964).
29. L. C. Thomas, R. A. Chittenden, and H. E. Hartley, *Nature* **192**, 1283 (1961).
30. G. S. Denisov and K. G. Tokhadze, *Dokl. Akad. Nauk* **337** (1), 54 (1994) [*Dokl. Phys. Chem.* **337**, 117 (1994)].
31. K. G. Tokhadze, G. S. Denisov, M. Wierzejewska, and M. Drozd, *J. Mol. Struct.* **404**, 55 (1997).
32. R. E. Asfin, G. S. Denisov, and K. G. Tokhadze, *J. Mol. Struct.* **608**, 161 (2002).
33. R. E. Asfin, G. S. Denisov, D. N. Poplevchenkov, *et al.*, *Pol. J. Chem.* **76**, 1223 (2002).
34. T. Haber, U. Schmitt, C. Emmeluth, and M. A. Suhm, *Faraday Discuss.* **118**, 331 (2001).
35. F. Ito and T. Nakanaga, *Chem. Phys.* **277**, 163 (2002).
36. M. Halupka and W. Sander, *Spectrochim. Acta A* **54**, 495 (1998).
37. Z. Mielke, K. G. Tokhadze, Z. Latajka, and E. Ratajczak, *J. Phys. Chem.* **100**, 539 (1996).
38. D. Hadzi and S. Bratos, in *The Hydrogen Bond. Recent Developments in Theory and Experiments*, Ed. by P. Schuster, G. Zundel, and C. Sandorfy (North-Holland, Amsterdam, 1976), pp. 565–611.
39. S. Bratos, H. Ratajczak, and P. Viot, in *Hydrogen Bonded Liquids*, Ed. by J. C. Dore and P. Teixeira (Kluwer Academic, New York, 1991), pp. 221–235.
40. J. T. Braunscholtz, G. E. Hall, F. G. Mann, and N. Sheppard, *J. Chem. Soc.*, No. 3, 868 (1959).
41. S. T. King, *J. Phys. Chem.* **74**, 2133 (1970).
42. S. G. Stepanian, I. D. Reva, E. D. Radchenko, *et al.*, *J. Mol. Struct.* **484**, 19 (1999).
43. J. Lundell, M. Rasanen, and Z. Latajka, *Chem. Phys.* **189**, 245 (1994).
44. L. Andrews and S. R. Davis, *J. Chem. Phys.* **83**, 4983 (1985).
45. Z. Mielke, Z. Latajka, J. Kolodziej, and K. Tokhadze, *J. Phys. Chem.* **100**, 11 610 (1996).
46. L. González, O. Mó, M. Yáñez, and J. Elguero, *J. Chem. Phys.* **109**, 2685 (1998).
47. F. Giordano and A. Ripamonti, *Acta Crystallogr.* **22**, 678 (1967).
48. D. Fenske, R. Mattes, J. Lons, and K. F. Tebbe, *Chem. Ber.* **106**, 1139 (1973).
49. K. A. Lyssenko, G. V. Grintselev-Knyazev, and M. Yu. Antipin, *Mendeleev Commun.* **12** (4), 128 (2002).
50. L. S. Khaikin, O. E. Grikin, A. V. Golubinskiĭ, *et al.*, *Dokl. Akad. Nauk* **390**, 791 (2003).
51. L. S. Khaikin, O. E. Grikin, L. V. Vilkov, *et al.*, *J. Mol. Struct.* **658**, 153 (2003).
52. R. L. Redington and K. C. Lin, *J. Chem. Phys.* **54**, 4111 (1971).
53. Y. Marechal, *J. Chem. Phys.* **87**, 6344 (1987).
54. G. M. Florio, E. L. Sibert III, and T. S. Zwier, *Faraday Discuss.* **118**, 315 (2001).
55. D. N. Shchepkin, Available from VINITI (Leningrad State Univ., 1987), No. 7511-B87.
56. V. P. Bulychiev, T. D. Kolomiitsova, and D. N. Shchepkin, *Opt. Spektrosk.* **76**, 730 (1994) [*Opt. Spectrosc.* **76**, 647 (1994)].

Translated by V. Rogovoi